



Apoptosis-inducing peptide loaded in PLGA nanoparticles induces anti-tumor effects *in vivo*

Dwi L. Priwitaningrum^{a,b}, Julian Jentsch^a, Ruchi Bansal^a, Sima Rahimian^c, Gert Storm^c, Wim E. Hennink^b, Jai Prakash^{a,*}

^a Targeted Therapeutics and Nanomedicine, Department of Biomaterials Science and Technology, Faculty of Science and Technology, University of Twente, Enschede, The Netherlands

^b Department of Pharmaceutics, Faculty of Pharmacy, University of Sumatera Utara, Medan, Indonesia

^c Department of Pharmaceutics, Utrecht Institute for Pharmaceutical Sciences, Faculty of Science, Utrecht University, Utrecht, The Netherlands

ARTICLE INFO

Keywords:

Cell penetrating peptide

Breast tumor

Polymeric nanoparticles

Nanomedicine

Peptide delivery

ABSTRACT

Induction of apoptosis in tumor cells specifically within the complex tumor microenvironment is highly desirable to kill them efficiently and to enhance the effects of chemotherapy. Second mitochondria-derived activator of caspase (Smac) is a key pro-apoptotic pathway which can be activated with a Smac mimetic peptide. However, *in vivo* application of peptides is hampered by several limitations such as poor pharmacokinetics, rapid elimination, enzymatic degradation, and insufficient intracellular delivery. In this study, we developed a nanosystem to deliver a Smac peptide to tumor by passive targeting. We first synthesized a chimeric peptide that consists of the 8-mer Smac peptide and a 14-mer cell penetrating peptide (CPP) and then encapsulated the Smac-CPP into polymeric nanoparticles (Smac-CPP-NPs). *In vitro*, Smac-CPP-NPs were rapidly internalized by 4T1 mammary tumor cells and subsequently released Smac-CPP into the cells, as shown with fluorescence microscopy. Furthermore, Smac-CPP-NPs induced apoptosis in tumor cells, as confirmed with cell viability and caspase 3/7 assays. Interestingly, combination of Smac-CPP-NPs with doxorubicin (dox), a clinically used cytostatic drug, showed combined effects *in vitro* in 4T1 cells. The effect was significantly better than that of SMAC-CPP-NPs alone as well as empty nanoparticles and dox. *In vivo*, co-treatment with Smac-CPP-NPs and free dox reduced the tumor growth to 85%. Furthermore, the combination of Smac-CPP-NPs and free dox showed reduced proliferating tumor cells (Ki-67 staining) and increased apoptotic cells (cleaved caspase-3 staining) in tumors. In conclusion, the present study demonstrates that the intracellular delivery of Smac-mimetic peptide using nanoparticle system can be an interesting strategy to attenuate the tumor growth and to potentiate the therapeutic efficacy of chemotherapy *in vivo*.

1. Introduction

Cancer cells have the ability to employ a number of different strategies to suppress the apoptotic response via multiple cell signaling mechanisms (Fandy et al., 2008; Plati et al., 2008; Fulda, 2010). Among others, inhibitors of apoptosis proteins (IAPs) are recognized as one of the major regulators of apoptosis (Barras and Widmann, 2011; Kocab and Duckett, 2016). Second mitochondria-derived activator of caspase (Smac) mitochondrial protein (also known as direct IAP binding protein with low pI, DIABLO) is released into the cytosol, blocks IAP and promotes caspase activity thereby stimulate cell apoptosis intrinsically (Mizukawa et al., 2006; Mao et al., 2013). Inhibition of this process is

also associated with the failure of chemotherapies to kill cancer cells (Ausserlechner and Hagenbuchner, 2016). Moreover, the Smac-mediated inhibition of IAP inducing apoptosis in tumor cells can be combined with chemotherapy to potentiate the efficacy by enhancing therapeutic effects and/or allowing use of lower doses of cytostatic chemotherapeutic drugs leading to reduced adverse effects (Mizukawa et al., 2006; Fandy et al., 2008; Danhier et al., 2010; Torchilin, 2011). Studies have shown that a small Smac mimetic i.e. AVPI (Ala-Val-Pro-Ile), a short N-terminal peptide of the Smac protein is essential for its binding to Baculoviral IAP Repeat 3 (BIR3) domain of IAPs to block their anti-apoptotic effect (Arnt et al., 2002; Fandy et al., 2008; Mao et al., 2013). Therefore, mimicking AVPI peptide to target IAPs

* Corresponding author at: Targeted Therapeutics and Nanomedicine, Department of Biomaterials Science and Technology, Faculty of Science and Technology, University of Twente, Zuidhorst ZH245, 7500 AE Enschede, The Netherlands.

E-mail address: j.prakash@utwente.nl (J. Prakash).

<https://doi.org/10.1016/j.ijpharm.2020.119535>

Received 21 March 2020; Received in revised form 4 June 2020; Accepted 6 June 2020

Available online 10 June 2020

0378-5173/© 2020 Elsevier B.V. All rights reserved.

represents a potential strategy for the treatment of cancer. However, use of peptides as therapeutics is limited due to several problems such as insufficient intracellular delivery, poor pharmacokinetics, rapid elimination, and enzymatic degradation (Jain et al., 2013; Bruno et al., 2013).

Cell-penetration peptides (CPPs) have been well reported to induce intracellular delivery of peptides (Jiao et al., 2009; Shin et al., 2014). CPPs, formerly known as protein transduction domains (PTD), are short peptides of less than 40 amino acids that are able to carry a variety of cargoes, including nucleic acids, antisense oligonucleotides, peptides, proteins, low molecular weight drugs, and nanoparticles to translocate across cell membrane (Rizzuti et al., 2015; Copolovici et al., 2014; Koppelhus et al., 2002; Nakase et al., 2013; Margus et al., 2012; Steinbach et al., 2016; Torchilin, 2008; Farkhani et al., 2014). CPPs have also been identified for their potential in mediating cell internalization, overcoming biological membrane for drug delivery which mainly involve endocytosis and transduction. Moreover, Smac-peptides have also been reported for their conjugation with different CPPs including antennapedia (Mizukawa et al., 2006), TAT (Du et al., 2013), and poly(arginine) (Chen et al., 2013) to enhance their intracellular delivery and tumor killing.

However, it should be noted that an intravenous administration of Smac-CPP will lead to unspecific uptake by any cell that comes in contact with Smac-CPP and may lead to many off-target than tumor-related effects. Therefore, we hypothesize that encapsulation of Smac-CPP into nanoparticles might be an interesting modality to deliver such peptides to tumors effectively, in order to protect the peptide from rapid degradation and to avoid interaction with healthy tissues. Also, nanoparticles tend to accumulate into tumors via the Enhanced Permeability and Retention (EPR) effect (Yang et al., 2003; Maeda, 2012; Maeda, 2015) and subsequently deliver the cargo i.e. Smac-CPP inside the tumor cells after internalization. However, it is essential that the released Smac-CPP peptide escapes from endosomes to elicit apoptosis-inducing effects in the cytosol. Studies have shown that CPPs assist in escaping from endosomes to reach the cytosol (Räägela et al., 2009; Danhier et al., 2012).

In the present study, we aimed to deliver Smac-CPP intracellularly using poly(lactic-co-glycolic acid) (PLGA) polymeric nanoparticles and examined the effect *in vitro* and *in vivo* in a mouse tumor model. First, we designed a chimeric peptide containing Smac-mimetic 8-mer peptide (AVPIAQKS) fused to an arginine-rich 14-mer CPP (VSRRRRRRG-GRRRR) that has been shown to have cell penetration activities (Park et al., 2005) and low toxicity in animal studies (Park et al., 2003). We subsequently confirmed that this 22-mer Smac-CPP chimeric peptide induces anti-tumor effects in triple negative 4T1 mouse breast tumor cells and that the combination with doxorubicin, a cytotoxic chemotherapeutic drug, led to the anticipated combined anti-tumor effects. We then loaded the Smac-CPP peptide into PLGA nanoparticles and investigated the intracellular uptake and anti-tumor effects of Smac-CPP nanoparticle formulation in 4T1 cells *in vitro*. Finally, Smac-CPP loaded PLGA nanoparticles with or without co-administered doxorubicin were examined for their anti-tumor effects *in vivo* in 4T1 orthotopic breast tumor model in mice.

2. Materials and methods

2.1. Materials

The Smac-CPP chimeric peptide was provided by China Peptides (Shanghai, China). Doxorubicin (Dox) was obtained from Sigma Aldrich (Zwijndrecht, the Netherlands) and stored in DMSO as a 10 mM stock solution at -20°C . RPMI-1640 without L-glutamine was purchased from PAA/GE Healthcare Life Sciences (Eindhoven, The Netherlands). L-Glutamine, penicillin/streptomycin, and calcium chloride were purchased from Sigma-Aldrich (Zwijndrecht, The Netherlands). Trypsin-EDTA 0.5% and fetal bovine serum (FBS) were purchased from Life

Technologies (Bleiswijk, The Netherlands). Cyanine 3 dye was purchased from Lumiprobe (Hannover, Germany). NucBlue™ Fixed Cell ReadyProbes™ Reagent was purchased from Thermo Scientific (Landsmeer, The Netherlands). Resazurin sodium salt used for alamar blue solution, propidium iodide, and haematoxylin were purchased from Sigma-Aldrich. SensoLyte® Homogeneous AMC Caspase-3/7 Assay Kit was obtained from Anaspec (Fremont, USA). eBioscience™ Annexin V-FITC (rh) was purchased from Life Technologies (Bleiswijk, The Netherlands). Sodium chloride was obtained from Merck (Amsterdam, The Netherlands). Uncapped PLGA (lactide/glycolide molar ratio 50:50, IV = 0.4 dl/g, Mw = 44,000 Da) was obtained from Corbion Purac (Gorinchem, The Netherlands). mPEG₂₀₀₀-PLGA₄₄₀₀₀ was synthesized by ring opening polymerization (Samadi et al., 2013). Buffered sodium chloride solution (NaCl 8.2 g, Na₂HPO₄·12H₂O 3.1 g, NaH₂PO₄·2H₂O 0.3 g in 1L of water for injection, pH 7.4) was from Braun (Melsungen AG, Germany). Ethyl acetate was purchased from VWR chemicals (Amsterdam, The Netherlands). Polyvinyl alcohol (PVA, Mw 30,000 – 70,000 Da) was purchased from Sigma Aldrich (Zwijndrecht, The Netherlands). Cryomatrix™ and 3-amino-9-ethyl-carbazole (AEC (red), Invitrogen), were purchased from Thermo Fisher Scientific (Landsmeer, The Netherlands). Rabbit anti-Ki-67 and Aquatex® aqueous mounting medium were acquired from Millipore-Merck (Amsterdam, The Netherlands). Rabbit anti-cleaved caspase-3 of Cell Signaling Technology was obtained from Bioké (Leiden, The Netherlands). (HRP)-labeled goat anti-rabbit IgG and rabbit anti-goat IgG were purchased from DAKO (Agilent, Amstelveen, The Netherlands). Milli-Q® water was obtained using Millipore Advantage A10 (Billerica, MA, USA). Phosphate buffer saline (PBS; NaCl 0.14 M, KCl 0.03 M, Na₂HPO₄ 0.08 M, NaH₂PO₄·H₂O 0.01 M, pH 7.4) was prepared in our lab. Mini Dialysis Kit 1 kDa was purchased from GE Healthcare Life Sciences. Slide-A-Lyzer™ G2 Dialysis Cassettes 2 kDa MWCO was acquired from Thermo Fisher Scientific.

2.2. Cell culture

Mouse 4T1 breast cancer cells were obtained from American Type Culture Collection (ATCC, Wessel, Germany). 4T1 cells were cultured in Roswell Park Memorial Institute (RPMI) 1640 medium supplemented with 2 mM L-glutamine, 10% fetal bovine serum and antibiotics (50 U/ml Penicillin and 50 µg/ml streptomycin). The cells were grown in cell culture treated 75 cm² flasks in a humidified incubator at 37 °C with 5% CO₂. Cells were passaged every 3 days and 0.05% trypsin-EDTA in PBS was used for cell detachment.

2.3. Characterization of the Smac peptide

The 22-mer Smac-CPP peptide construct was designed by our lab, and was synthesized and characterized by China Peptides. Ultra High Performance Liquid Chromatography (UHPLC) analysis was performed using a Kromasil 100-5C18 Column (4.6 mm × 150 mm, 5 µm) and ultraviolet detection at wavelength of 220 nm. The mobile phase was consisted of 0.1% TFA in water (solvent A) and 0.1% TFA in acetonitrile (solvent B). A linear gradient was applied from 5 to 35% solvent B in 16 min, with elution flow rate 1 ml/min. Mass analysis was done using a Mass Spectrometer API 150 EX (Perkin Elmer, USA).

2.4. Polymer characterization

¹H NMR analysis of the mPEG-conjugated polymer (mPEG-PLGA) was conducted by dissolving sample in DMSO-*d*₆. The molar % of composing units (%PEG, %L, lactic acid; and %G, glycolic acid) were determined by ¹H NMR, according to the following formulas:

$$I_G = (I_{4.7-5.0})/2$$

$$I_L = (I_{1.3-1.5})/3$$

$$\%L = \frac{I_L}{I_L + I_G} \times 100\%$$

$$\%G = \frac{I_G}{I_L + I_G} \times 100\%$$

where I_G and I_L = peak integrals per one proton of each monomer unit, I_{number} is the integral obtained from the NMR spectra at the indicated peak shifts (ppm).

Molecular weight of diblock copolymers = $(I_L/I_{\text{PEG}} \times \text{MW Lactic acid}) + (I_G/I_{\text{PEG}} \times \text{MW Glycolic acid}) + \text{MW PEG}$. I_{PEG} is the peak integral per one proton of PEG

$\% \text{PEG} = \text{PEG molecular weight/calculated diblock molecular-weight} \times 100\%$

2.5. Preparation of Smac-CPP-loaded PLGA nanoparticles

PLGA nanoparticles (NPs) were prepared by a double emulsion solvent evaporation method as described previously with minor adjustments (Samadi et al., 2013; Li et al., 2001; Cho and Sah, 2005). Briefly, the internal water phase, which was 100 μL of 10 mg/mL Smac-CPP solution in buffered sodium chloride solution (NaCl 8.2 g, $\text{Na}_2\text{HPO}_4 \cdot 12\text{H}_2\text{O}$ 3.1 g, $\text{NaH}_2\text{PO}_4 \cdot 2\text{H}_2\text{O}$ 0.3 g in 1 L of water for injection, pH 7.4), was emulsified in 2 mL of 2% ethyl acetate containing 30% (w/w) mPEG₂₀₀₀-PLGA blended with PLGA (lactide/glycolide molar ratio 50:50, IV = 0.4 dL/g, molecular weight of 44,000 Da), the total polymer concentration was 2.5% w/v. The emulsification was performed in an ice-bath using an ultrasonic homogenizer (Branson Sonifier 250, Branson Ultrasonics Corporation, Danbury, USA) for 30 s at 10% power output. Subsequently, the formed w/o emulsion was added to an external aqueous phase of 2 mL of 2% PVA (w/v) (Mw 30,000 – 70,000 Da). A water-in-oil-in-water (w/o/w) emulsion was subsequently formed by sonication for 1 min at 10% power output. Next, the double emulsion was transferred into 45 mL of 0.3% PVA (w/v), and stirred overnight at room temperature to allow evaporation of ethyl acetate and to solidify the emulsified droplets. Nanoparticles were collected by centrifugation for 20 min at 20,000 rpm (Rotor SS-34, Sorvall RC-5C Plus, Kendro Lab, USA), and the supernatant was discarded. Finally, the particles were washed with 30 mL of PBS and water, and lyophilized. To prepare empty NPs and Cyanine 3 dye (Cy3)-labeled Smac-CPP loaded NPs, 100 μL PBS solution and 100 μL of Cy3-Smac-CPP were added as internal water phase, respectively. Lyophilized Smac-CPP-loaded NPs were subsequently labeled with Cy3 for *in vitro* uptake study as described in Section 2.7.3.

2.6. Characterization of placebo and Smac-CPP-loaded PLGA nanoparticles

2.6.1. Size and zeta potential

The obtained empty (placebo) and Smac-CPP-loaded NPs were characterized for size and zeta potential using a Nano ZS Zetasizer (Malvern Instruments, Malvern, UK) at 20 °C. Nanoparticles were suspended in Milli-Q® water (100 $\mu\text{g/mL}$), and their average size and size distribution was determined by dynamic light scattering (DLS). The Z-average size was analyzed using cumulants and CONTIN approaches and reported using intensity distribution value. Nanoparticles dispersion of 100 $\mu\text{g/mL}$ in 10 mM KCl pH 6.0 was injected into a folded capillary cell DTS 1070 (Malvern Instruments, UK) for zeta potential measurements and analyzed using Smoluchowski approach.

2.6.2. Morphology

The morphology of the nanoparticles was imaged using Scanning Electron Microscopy (SEM, JEOL JSM-IT100 InTouchScope™, USA). A diluted nanoparticle suspension in water was placed onto the 12 mm diameter aluminum stub, covered with conductive carbon adhesive tape (Electron Microscopy Sciences, Pennsylvania, USA) and left overnight to dry. Samples were sputtered with gold under vacuum.

2.6.3. Peptide content and loading efficiency of Smac-CPP-loaded PLGA NPs

The peptide loading and encapsulation efficiency were determined by analyzing digested nanoparticle samples using reversed-phase UHPLC, as reported previously (Silva et al., 2013). In brief, 10 mg of lyophilized Smac-CPP-loaded NPs was dissolved in 250 μL of DMSO and incubated at 50 °C and agitated at 400 rpm for 30 min. Next, 750 μL of 50% ACN in Milli-Q® water with 0.1% TFA was added. The mixture was incubated at 50 °C for additional 6 h at 400 rpm to allow dissolution of the peptide and degradation/precipitation of the polymer. The precipitated polymer was separated from the dissolved peptide by centrifugation for 20 min at 20,000g. The supernatant containing the peptide was collected and subsequently 20 μL was injected and analyzed with UPLC (Thermo Scientific™ UltiMate™ 3000 BioRS System). The UPLC system was equipped with an Acquity UPLC CSH C18 Column (130 Å, 1.7 μm , 2.1 mm \times 150 mm) and an ultraviolet detector (Diode Array, Dionex, Thermo Scientific) at 214 nm. The mobile phase consisted of 5% acetonitrile in Milli-Q® water with 0.1% TFA (solvent A) and 95% acetonitrile in Milli-Q® water containing 0.1% TFA (Solvent B). A linear gradient was applied from 0% to 33% solvent B, at a flow rate of 0.4 mL/min. Peptide content was calculated using a calibration curve obtained by injection of samples known concentrations of Smac-CPP (4.7 to 300 $\mu\text{g/mL}$). The encapsulation efficiency (EE) is defined as the amount of peptide entrapped divided by the feeding peptide \times 100%. Loading efficiency (LE) is defined as the encapsulated amount of peptide divided by dry weight of loaded-nanoparticles \times 100%.

2.6.4. Peptide release from nanoparticles

The release of the Smac-CPP from the NPs was studied in buffer (PBS pH 7.4, NaCl 0.14 M, KCl 0.03 M, Na_2HPO_4 0.08 M, $\text{NaH}_2\text{PO}_4 \cdot \text{H}_2\text{O}$ 0.01 M) containing 0.05% (w/v) NaN_3 . Samples of freshly prepared nanoparticles were suspended in PBS (10 mg/mL) and aliquoted into low-peptide binding tubes (Sarstedt, Nümbrecht, Germany). The samples were incubated at 37 °C under mild agitation and at different time points, one tube was taken and centrifuged at 22,000g for 20 min. The obtained supernatant was stored at –20 °C until measurement. The amount of peptide released in the supernatant was measured using UHPLC (as described in Section 2.6.3). The amount of released peptide was calculated relative to the loaded amount of peptides present in the suspended particles.

2.7. *In vitro* cellular uptake of Smac-CPP and Smac-CPP loaded PLGA NPs

2.7.1. Labeling Smac-CPP with Cyanine 3 dye

The Smac-CPP was labeled with Cyanine 3-NHS ester (Cy3-NHS) for uptake study (Li et al., 2015) for cellular uptake studies. In short, the Smac-CPP peptide was dissolved in PBS (30 mg/mL) and subsequently to 100 μL of this solution, 100 μL of Cy3-NHS dissolved in DMSO (10 mg/mL) was added (1:1 M ratio peptide/dye). The reaction was allowed to proceed for 16 h at 4 °C. The resulting Cy3-labeled Smac-CPP peptide was dialyzed against PBS using a Mini Dialysis Kit 1 kDa or Slide-A-Lyzer™ G2 Dialysis Cassettes 2 kDa MWCO at 4 °C. The resulting Cy3-labeled peptide was dissolved in PBS (100 μM) and stored at 4 °C.

2.7.2. *In vitro* cellular uptake of Smac-CPP

4T1 cells were seeded in a 24-well plate (1×10^4 cells/well) in RPMI-1640 medium supplemented with 2 mM L-glutamine, 10% fetal bovine serum and antibiotics (50 U/mL penicillin and 50 $\mu\text{g/mL}$ streptomycin), and incubated for 24 h in a humidified incubator at 37 °C with 5% CO_2 . Next, 5 μL of Cy3-labeled Smac-CPP dissolved in PBS (final concentration was 5 μM) was added. After 2 and 18 h incubation, the cells were evaluated using fluorescence imaging. Next, the cells were washed with PBS and subsequently fresh medium was added. The nuclei were visualized by applying NucBlue™ Fixed Cell ReadyProbes™ Reagent containing DAPI. The uptake of Cy3-labeled Smac-CPP was

imaged 20 min after nuclei staining at room temperature. Cy3-label (Ex/Em 555/570 nm) and nuclei were detected through Texas Red and DAPI filter, respectively, using EVOS® FL Color Imaging System (Life Technologies).

2.7.3. *In vitro* cellular uptake of Smac-CPP loaded PLGA NPs and Cyanine-3 labeling

Fluorescence imaging was performed to detect the cellular uptake of Smac-CPP loaded NPs. In this study, two labeled formulations were prepared: one with the label linked to the peptide and the other with the label bound onto the surface of the PLGA NPs. Firstly, Smac-CPP was labeled with Cy3-NHS as described in Section 2.7.1, and subsequently this labeled peptide was loaded in NPs yielding (Cy3-Smac-CPP)-NPs using the same procedure as described in Section 2.5. Secondly, Smac-CPP-loaded NPs were labeled with Cy3 prepared using carbodiimide chemistry via EDC/NHS activation yielding Cy3-NP-(Smac-CPP). In short, 50 µl of a solution of 40 mM EDC/NHS in MES Buffer (0.5 M, 975 mg MES hydrate in 10 ml Milli-Q® water, adjusted to pH 6.3 with Na₂CO₃ 2.5 M) was added to 200 µl loaded-nanoparticles suspension (25 mg/ml) and allowed to react for 45 min at room temperature. Next, the formed activated nanoparticles were resuspended in 200 µl of PBS and reacted with 10 µl of Cy3-amine in DMF (10 mg/ml) for 2 h at room temperature. The resulting Cy3-conjugated Smac-CPP-loaded PLGA nanoparticles (Cy3-NP-(Smac-CPP)) were purified using an Amicon® column by washing with PBS thrice, resuspended in PBS (25 mg/ml), and stored at 4 °C.

4T1 cells were pre-incubated with labeled formulations for 2 h at 37 °C. The medium with the labeled nanoparticles was removed after 2 h, and the cells were subsequently incubated with 4T1 cell-medium alone for next 18 h and thereafter visualized using fluorescence microscopy, as described above.

2.8. Cell viability assay

Cell viability assay was performed using Alamar Blue assay to investigate the dose–response of 4T1 cell viability towards Smac-CPP. 4T1 cells were seeded at a density of 2500 cells per well in a 96-well plate. After 24 h of incubation in RPMI-1640 medium supplemented with 2 mM L-glutamine, 10% fetal bovine serum and antibiotics (50 U/ml Penicillin and 50 µg/ml streptomycin) in which Smac-CPP was dissolved (concentrations ranging from 5 to 1000 µM), the cells were incubated for 48 h in a humidified incubator at 37 °C with 5% CO₂.

The combined effects of doxorubicin and Smac-CPP on the viability of 4T1 cell was also investigated. Briefly, 4T1 cells were pre-incubated with Smac-CPP (final concentration was 100 µM) for 4 h prior to doxorubicin (concentrations ranging from 0 to 10,000 nM), and incubated for an additional 48 h.

Cell viability assay was also performed to investigate the efficacy of Smac-CPP loaded in PLGA in the absence and presence of doxorubicin. 4T1 cells were pre-incubated with Smac-CPP-loaded NPs at a peptide dose of 0, 50, and 100 µM for 16 h in a humidified incubator at 37 °C with 5% CO₂ to allow the release of the peptide release from the nanoparticles, and subsequently doxorubicin (final concentration was 100 nM) was added and the cells were incubated for additional 48 h. As comparison, 4T1 cells were incubated only with Smac-CPP-loaded NPs at a peptide dose of 0, 50, 100 µM for 16 h for additional 48 h. At the same time, empty nanoparticles were also incubated (in the same concentration as used for peptide-loaded nanoparticles) with the cell to assess possible cytotoxic effects.

After each of the prior described treatments, 110 µl of Alamar Blue solution (440 µM resazurin salt in PBS, diluted 1:10 v/v in RPMI medium) was added to the wells and the cells were incubated for additional 4 h at 37 °C. Fluorescence of reduced resazurin was subsequently measured using Victor³ 1420 Multilabel Counter (Perkin Elmer, USA) at excitation/emission 560/590 nm. The cell viability ratio was calculated as following equation: cell viability (%) = (the absorbance

of treated cells in medium – absorbance of medium only)/(absorbance of non-treated cells in medium – absorbance of medium only) × 100%.

2.9. Apoptosis assay

Cell apoptosis was investigated by performing Caspase 3/7 assay and Annexin V-FITC staining (Schimmer et al., 2004).

2.9.1. Caspase 3/7 assay

4T1 cells were seeded at a density of 2500 cells/well in a 96-well plate and incubated in 4T1 medium as described in Section 2.2 in a humidified incubator at 37 °C with 5% CO₂ for 24 h prior to addition of Smac-CPP (20, 50, and 100 µM of free peptide). The cells were subsequently investigated for Caspase-3/7 activity after 48 h using a Caspase-3/7 assay kit as described in the manufacture instructions. The cells were also investigated for combination therapy of Smac-CPP-loaded NPs and doxorubicin. Smac-CPP-loaded NPs dispersed in PBS were added to the cells at a final peptide concentration of 100 µM when cells just attached to culture flask and incubated for 16 h at 37 °C. Subsequently, doxorubicin was added (final concentration was 0 and 100 nM) and the cells were incubated for 48 h after which the Caspase 3/7 assay was carried out.

2.9.2. Annexin V-FITC staining

Annexin V staining was performed to visualized early apoptosis of cells induced by Smac-CPP. 4T1 cells were seeded at a density of 3×10^4 cells/well in 24-well plate and incubated for 6 h until the cells just attached to the culture flask. Next, 35 µl of a dispersion of Smac-CPP-loaded NPs (final concentration of the peptide was 100 µM) for 16 h at 37 °C and subsequently, doxorubicin was added (final concentration was 100 nM) and incubated for another 2 h. 4T1 cells were incubated for 16 h to achieve release of the Smac-CPP peptide from nanoparticles. The cells were also pre-incubated with 100 µM of Smac-CPP for 4 h, and subsequently doxorubicin was added (final concentration was 100 nM) and the cells were incubated for another 2 h prior to performing the Annexin V-FITC staining. As control, cells were incubated with 100 µM of Smac-CPP only, and cells incubated with medium only.

After each of the prior described treatments, cells were washed with binding buffer containing 10 mM Hepes (pH 7.4), 140 mM NaCl and 2.5 mM CaCl₂. Next, 25 µl of Annexin V FITC solution (1:40 in binding buffer) and 25 µl of propidium iodide solution (100 µg/ml in water) were added to 950 µl of binding buffer and, 500 µl of this solution was added to each well and the cells were incubated at room temperature for 15 min. Subsequently, the cells were washed with binding buffer only and fixated with 50 µl paraformaldehyde and incubated at room temperature for 15 min. Fixed cells were subsequently washed with binding buffer and stained for nuclei with DAPI-mounting medium. Cells were imaged immediately using fluorescence microscopy (Nikon). Annexin V-FITC bound to phosphatidylserine on the outer leaflet of cell membranes was detected using fluorescence microscopy (Nikon) with 20× and 40× magnification through FITC filter. PI, showing the dead cells, was detected through Rhodamine filter (Ex/Em 540/570 nm) or Texas Red filter (Ex/Em 590/610 nm).

2.10. Antitumor efficacy of Smac-CPP-loaded PLGA NPs in combination with doxorubicin in orthotopic 4T1 mouse breast tumor model

All experimental procedures were approved by the animal experimental committee of Utrecht University, The Netherlands. Mouse breast 4T1 tumor cells (100,000 cells in PBS/mouse, injection volume of 50 µl) were injected subcutaneously in the mammary fat pad of the Balb/c mice (Janvier Labs, Le Genest-Saint-Isle, France) under anesthesia. When the tumor reached a size of about 100 mm³, the mice were injected intravenously through tail's vena (injected volume of 150 µl)

with Smac-CPP-loaded NPs (at peptide dose of 20 mg/kg), doxorubicin (2.5 mg/kg), Smac-CPP-loaded NPs (peptide dose of 20 mg/kg) + free doxorubicin (2.5 mg/kg), and PBS (6 mice per group), twice a week for 3 weeks. Tumor size was measured twice weekly using Vernier caliper to calculate tumor volume using formula i.e. $\text{length} \times \text{width}^2 \times 0.5$. The body weights of the mice were also measured during tumor measurements. Animals were euthanized under anesthesia when the tumor became 1000 mm³. Tumors were harvested for histology and subjected to immunohistochemical staining's for proliferation and apoptosis markers, Ki-67 and cleaved caspase 3, respectively.

2.11. Immunohistology

Tumors harvested from the *in vivo* study were frozen in Cryomatrix™ and stained for analyzing proliferation and apoptosis marker. Frozen tumors were cut into 6 µm-thick sections and processed for immunostaining. Cryosections were first fixed with acetone at room temperature (RT) for 15 min, rehydrated in PBS and incubated with either rabbit anti-Ki-67 (1:100) or rabbit anti-cleaved-caspase 3 (Asp175) (1:300) in PBS for 1 h at RT. Subsequently, sections were washed with PBS and incubated with secondary antibody-horseradish peroxidase (HRP)-labeled goat anti-rabbit IgG (1:100) in PBS for 1 h. Sections were subsequently washed with PBS and finally incubated with a tertiary antibody – HRP-labeled rabbit anti-goat IgG (1:100) in PBS for 1 h. The peroxidase activity was developed with 3-amino-9-ethyl-carbazole (AEC, red) in Milli-Q® water for 20 min. Next, the samples were counterstained with Haematoxylin to visualize cell nuclei, washed in running tap-water for 5 min, and mounted with Aquatex® aqueous mounting medium. Imaging was performed using Nanozoomer-RS. To quantify the staining, single tumor sections at a 20x magnification were analyzed using ImageJ software (ImageJ, NIH, USA) at a fixed threshold.

3. Results and discussions

3.1. Smac-CPP peptide and *in vitro* uptake

The Smac peptide AVPIAQKS is not able to penetrate through the cell membrane as well as the endosomal membrane (Du and Stenzel, 2014; Li et al., 2015). Therefore, in this study, a chimeric peptide

containing the sequence of the Smac peptide (AVPIAQKS) and CPP (VSRRRRRRGRRRR), as illustrated in Fig. 1A, was obtained by solid phase synthesis. The peptide had a purity > 97% and a molecular mass of 2675 Da as shown using UHPLC analysis and mass spectrometry respectively (Figs. S1 and S2). The isoelectric point (pI) of the peptide is 13.06 (calculated using peptide calculator at <http://pepcalc.com/peptide-solubility-calculator.php>). We first investigated whether Smac-CPP construct could be internalized by 4T1 breast tumor cells. To track the uptake, we labeled Smac-CPP with Cyanine 3 dye (Cy3) to form Cy3-Smac-CPP. As shown in Fig. 1B, a strong red fluorescence was observed at the cellular membrane or inside the cells in a dotted pattern, which is a typical indicator for the accumulation into endosomes. At 18 h, the accumulation increased remarkably and the fluorescence was localized near the nuclei, indicating that Smac-CPP can penetrate into through the cell membrane and potentially escape from the endosomes. These data are in line with other studies which showed that the CPP can induce cell penetration of different cargos via cell membrane (Conner and Schmid, 2003) and also escape through endosomes (van den Berg and Dowdy, 2011).

3.2. *In vitro* effect of Smac-CPP on 4T1 cell viability

The effect of Smac-CPP on the cell viability in 4T1 cells was examined using alamar blue assay. It was found that Smac-CPP reduced the viability of these cells in a dose-dependent manner, as shown in Fig. 2A, revealing IC₅₀ of 132 µM. Furthermore, it was investigated whether Smac-CPP shows a synergetic/combined cytotoxic effect of doxorubicin in these cells. Therefore, first the effect of doxorubicin on the viability of 4T1 cells was examined and a dose-dependent inhibition of cell viability was observed (Fig. 2B). To examine possible synergistic/combined effects of the Smac-CPP, solutions with a fixed concentration of 100 µM, which is close to the IC₅₀ value of the peptide (132 µM), and a varying concentrations of doxorubicin were incubated with the cells. We found that the combination treatment of Smac-CPP with doxorubicin resulted in an enhanced cytotoxic effect (Fig. 2B). In this case, a combined effect was significantly observed at lower doxorubicin concentrations, rather than synergistic effect, as the IC₅₀ of the combination treatment was not decreased when compared to single treatment of doxorubicin (IC₅₀ of 166 µM and 137 µM, respectively).

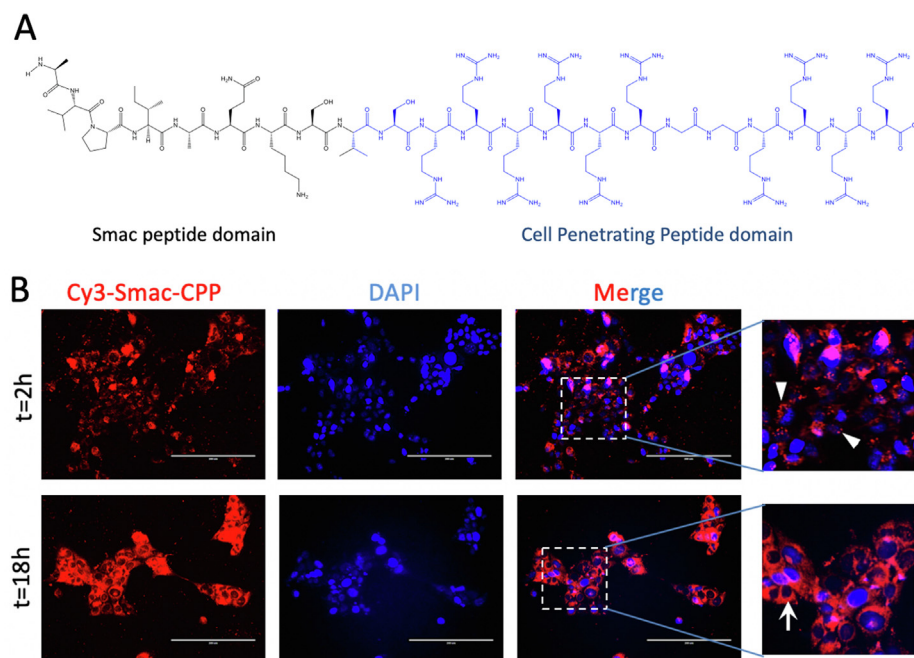


Fig. 1. Smac-CPP peptide and *in vitro* uptake into 4T1 tumor cells. (A) Chemical structure of the Smac peptide (AVPIAQKS) fused with CPP (VSRRRRRRGRRRR). (B) Representative fluorescence microscopic images showing cellular uptake of Cy3-labeled Smac-CPP (red) in 4T1 cells after 2 and 18 h incubation at 37 °C. The nuclei were stained with DAPI (blue). Scale bar: 50 µm.

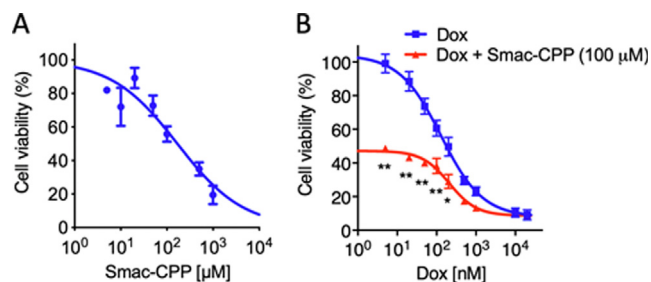


Fig. 2. Effect of Smac-CPP chimeric peptide in 4T1 tumor cells. The effect of Smac-CPP alone (A) and in combination with doxorubicin (Dox) (B) on the viability of 4T1 breast tumor cells. 4T1 cells were incubated with Smac-CPP only (range concentrations of 5 to 1000 μM) for 48 h. In combination therapy, 4T1 cells were pre-incubated with Smac-CPP (final concentration of 100 μM) for 4 h prior to doxorubicin (range concentrations of 0 to 10,000 nM), and incubated for an additional 48 h. Cell viability was determined using Alamar Blue assay. Mean \pm SEM from at least three independent experiments. Significance is denoted as * p < 0.05, ** p < 0.01 versus Dox.

3.3. The preparation and characterization of the peptide-loaded PLGA NPs

As Smac-CPP might interact with any cell type with which it comes in contact with, the peptide was encapsulated into PLGA nanoparticles (Smac-CPP NPs; Fig. 3A). PLGA nanoparticles have been extensively used for the intracellular delivery of proteins and peptides (Patel et al., 2014; Du and Stenzel, 2014; Samadi et al., 2014; Hirota et al., 2016; Faisant et al., 2002; Giteau et al., 2008). In this study, Smac-CPP NPs were prepared by a w/o/w double emulsion method which yielded particles with a yield of 85%, and an average diameter of 197 nm with a

polydispersity index (PDI) of 0.10 ± 0.01 , while corresponding placebo (empty) NPs were slightly smaller and had size of about 150 nm and PDI of 0.07 ± 0.02 (Table 1, Fig. 3B). The zeta potential of the peptide-loaded NPs was slightly more positive than that of empty NPs (-16 ± 3 versus -23 ± 11 mV) which might be explained by the presence of positive peptides at the surface of the particles. These negative value of zeta potential can be ascribed to carboxylate-end group (COO⁻) of PLGA polymer in spite of PEG content of 4.5%wt (Table S4) which corresponds with the previous studies (Xu et al., 2015; Gholizadeh et al., 2018; Martínez-Jothar et al., 2018). UHPLC analysis showed that the encapsulation efficiency (EE) of Smac-CPP was 48% and its corresponding loading capacity (L) was 2.4%. This relative high loading efficiency might be ascribed to the pH since at pH 7.4, the positively charged CPP, likely, interacts electrostatically with the terminal negatively charged COO⁻ groups of uncapped PLGA.

The molar ratio of PLGA-COOH and Smac-CPP peptide was calculated by assuming that one mol of polymer interacts with one mol of peptide. The functional group NH₂ at the N-terminal likely electrostatically interacts with the terminal negatively charged COO⁻ groups of uncapped PLGA since it has minimal steric hindrance. 100 μl of 10 mg/mL Smac-CPP solution was emulsified in 2 ml ethyl acetate containing 30% mPEG₂₀₀₀-PLGA blended with PLGA (lactide/glycolide molar ratio 50:50, IV = 0.4 dL/g, molecular weight of 44,000 g/mol) that resulted in a total polymer concentration of 2.5% w/v. There were 35 mg of PLGA (MW: 44000 g/mol) and 15 mg of mPEG₂₀₀₀-PLGA in the formulation which gave:

$$\left(\frac{0.035\text{g}}{44000\text{g/mol}} \right) + \left(\frac{0.015\text{g}}{46000\text{g/mol}} \right) = 1.12 \times 10^{-6} \text{ mol of polymer,}$$

and 100 μl of 10 mg/mL Smac-CPP solution gave

$$\left(\frac{0.001\text{g}}{2675.18\text{g/mol}} \right) = 3.74 \times 10^{-7} \text{ mol of peptide}$$

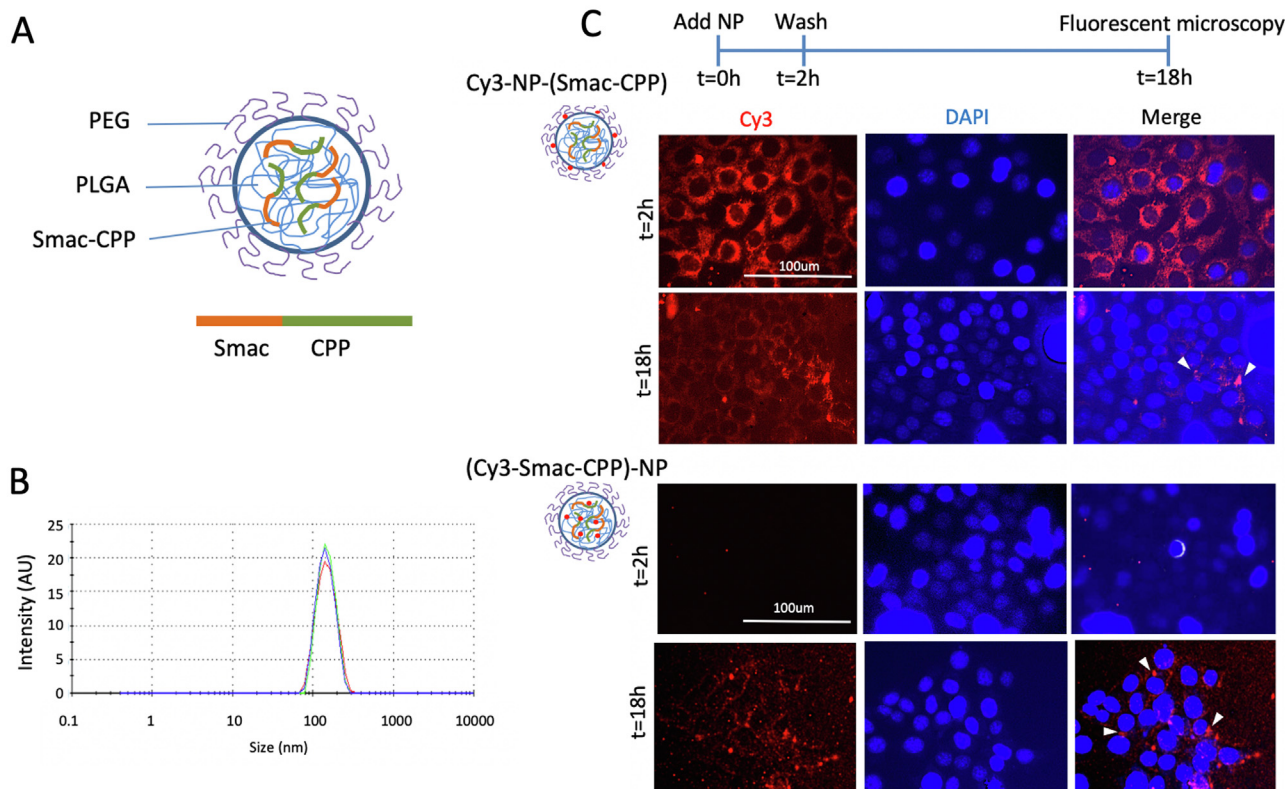


Fig. 3. Uptake of Smac-CPP PLGA nanoparticles by 4T1 tumor cells. (A) Schematic figure of Smac-CPP-loaded PLGA NPs. (B) Dynamic light scattering histogram showing the size distribution of Smac-CPP PLGA NPs. (C) Representative fluorescent microscopic images showing cellular uptake of Cy3-labeled PLGA NPs (either the label was coupled to the surface of the NPs, Cy3-NP-(SMAC-CPP) (top) or the peptide was loaded, (Cy3-SMAC-CPP)-NP (bottom)) by 4T1 cells after early (2 h) and late (18 h) time points. Cy3-staining is shown as red color. The nuclei were stained with DAPI (blue). Scale bar: 100 μm.

Table 1
Characteristics of PLGA nanoparticles with and without Smac-CPP peptide loading (n = 3).

Nanoparticles	Size (nm)	PDI	Zeta potential (mV)	Yield (%)	EE (%)	L (%)
placebo NPs	149 ± 15	0.07 ± 0.02	− 23 ± 11	88 ± 1	–	–
Smac-CPP NPs	197 ± 9	0.10 ± 0.01	− 16 ± 3	85 ± 10	48 ± 2	2.4 ± 0.01

PDI: polydispersity index, EE: encapsulation efficiency, L: loading capacity.

Thus, molar ratio of PLGA-COOH/peptide in the final formulation was $\left(\frac{1.12 \times 10^{-6}}{3.74 \times 10^{-7}}\right) = \frac{2.995}{1} \approx 3/1$

3.4. Cellular uptake of Smac-CPP NPs by 4T1 cells

Further, it was examined whether Smac-CPP NPs are internalized by 4T1 cells and as a result the Smac-CPP peptide was released inside the cells. To track the nanoparticles, the Smac-CPP loaded NPs were labelled at the surface with Cy3 dye using carbodiimide chemistry [Cy3-NP-(Smac-CPP)]. On the other hand, to track the peptide, the Smac-CPP peptide was labeled with Cy3 and then encapsulated into NPs resulting into (Cy3-Smac-CPP)-NP. Both Cy3-NP-(Smac-CPP) and (Cy3-Smac-CPP)-NP were incubated with 4T1 cells for 2 h, washed and then the cells were examined at 2 h and 18 h using a fluorescence microscope. As shown in Fig. 3C, Cy3-NP-(Smac-CPP) were rapidly internalized by 4T1 cells after 2 h of incubation and subsequently localized within cytosol. In spite of negative zeta potential of PLGA NPs which does not favor cellular uptake of nanoparticles (Sahay et al., 2010; Jain and Stylianopoulos, 2010), this result is in agreement with our previous study using charged nanoparticles (Priwitaningrum et al., 2016) as well as shown by Gao et al. (2013) and Rahimian et al. (2015a,b). Additionally, Joshi et al. (2013) showed that nanometer-sized PLGA NPs were more effectively taken up by the cells compared to micrometer sized particles. Wilhelm et al. (2003) also reported that anionic particles were internalized efficiently due to non-specific interaction with cell membrane and allowing nanoparticles uptake on cationic sites of plasma membrane. Furthermore, for (Cy3-Smac-CPP)-NP, fluorescence signal was not visible at t = 2 h which is likely due to quenching of the encapsulated labelled peptide. Interestingly, fluorescence was observed at 18 h, as can be seen in a dotted pattern (arrowheads) which might be ascribed to the release of Cy3-Smac-CPP intracellularly, that also seemed to be localized in the cytosol (Fig. 3C bottom). We tried to study the fluorescent in encapsulated NPs versus released peptide, however, the process to release the peptide completely is too harsh for intactness of the peptide and the dye. Furthermore, NPs themselves show a high interference during the fluorescence measurement. Although the detailed mechanism of intracellular release is yet to be studied, we expect that CPP might have induced the escape which has been shown earlier in other studies for the used CPP (El-Sayed et al., 2009; Takeuchi and Futaki, 2016).

3.5. The effects of Smac-CPP-loaded PLGA NPs on 4T1 viability in vitro

To demonstrate that the released Smac-CPP from PLGA NPs is able to induce apoptosis in tumor cells, we performed cell viability assays after incubation of 4T1 cells with Smac-CPP NPs. In addition, we combined the Smac-CPP NPs with doxorubicin to study potential additive effects (Fig. 4A). Interestingly, Smac-CPP NPs reduced the 4T1 cell viability in a similar manner as the free Smac-CPP (Fig. 4A versus Fig. 2A). Although the release of the peptide (in PBS) is very slow (only 2% of the loaded peptide during 2 days of incubation in PBS pH 7.4, see Fig. S3) the results of Fig. 4A suggest that the peptide is rapidly released from the PLGA-NPs after their cellular internalization, followed by a subsequent release from endosomes. We expect that after the release of Smac-CPP from NPs, CPP leads to a rapid release from endosomes which allows for an escape from the degradation. However, the mechanism for the release from PLGA-NPs and escape of the released

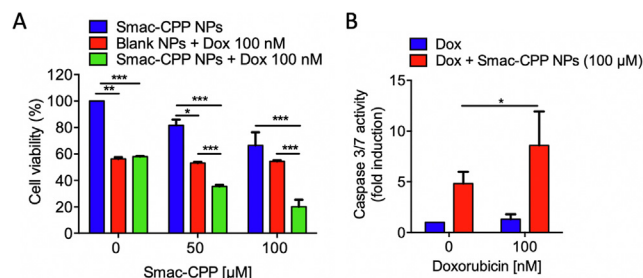


Fig. 4. Effects of Smac-CPP-loaded PLGA NPs in combination with doxorubicin (Dox) on the viability of 4T1 tumor cells. (A) Cell viability of 4T1 cells after 48 h of the combination treatment. Mean ± SEM, n = 3 and each experiment was performed in triplicate. *p < 0.05, **p < 0.01, ***p < 0.001. (B) Caspase 3/7 enzyme activity in 4T1 cells incubated with either Smac-CPP NPs (100 μM), Dox (100 nM) or both for 48 h. Mean ± SEM, n = 3. *p < 0.05.

peptide from endosome needs to be further investigated. Such faster intracellular releases of drugs from PLGA NPs had been reported previously (Verderio et al., 2013; Gomes dos Rios et al., 2019). When combined with doxorubicin (100 nM), Smac-CPP NPs (equivalent to Smac-CPP at 100 μM) substantially reduced the cell viability to nearly 80% compared to the viability of the cells upon incubation with Smac-CPP NPs only, as well as upon incubation with 100 nM doxorubicin in combination with empty nanoparticles. No effect from empty-NPs were observed from this study.

To prove whether the effects on the cell viability were due to induction of apoptosis, apoptosis assays i.e. caspase 3/7 enzyme activity assays and Annexin-V/propidium iodide (PI) co-stainings (Figs. 4B and 5) were performed. The results of the caspase 3/7 bioluminescence assay showed that incubation of 4T1 cells with Smac-CPP NPs significantly induced apoptosis compared to doxorubicin that showed only a small induction (Fig. 4B). Although doxorubicin is known to induce apoptosis (Pilco-Ferreto and Calaf, 2016), apoptosis induction was not observed in performed caspase enzyme assay. This might be due to the longer incubation period (48 h) at which doxorubicin-induced apoptosis was not detectable anymore (Balderson et al., 2019). A study by Balderson et al. (2019) showed that doxorubicin-induced caspase-3 activation peak occurred at 22 h after incubation of the cells with the drug. However, remarkably, the combination of doxorubicin with Smac-CPP NPs showed an enhanced effect, compared to either Smac-CPP NPs or free doxorubicin after 48 h incubation. These results can be explained by an efficient internalization of Smac-CPP NPs and intracellular release of the peptide. Besides that, Smac-CPP shows a combined effect with doxorubicin in 4T1 cells, as shown in Fig. 2B.

In order to capture early apoptosis events, annexin-V-FITC staining combined with propidium iodide was performed (to detect dying cells) after incubation for 2 h (Fig. 5). It was found that incubation of cells with doxorubicin alone for 2 h and Smac-CPP NPs alone for 16 h revealed an early apoptosis event, indicated by the positive stain for annexin-V-FITC and negative DNA-stain for PI (Fig. 5). Compared to caspase 3/7 assay in Fig. 4B, doxorubicin treated cells had much higher signal of annexin-V-FITC, which could be attributed to the differences in the sensitivity of the assays, duration of incubation and types of read out. Incubation of Smac-CPP NPs with cells for only 2 h did not show any positive staining (data not shown) indicated that there was no release of Smac CPP. Interestingly, combination of Smac-CPP NPs and

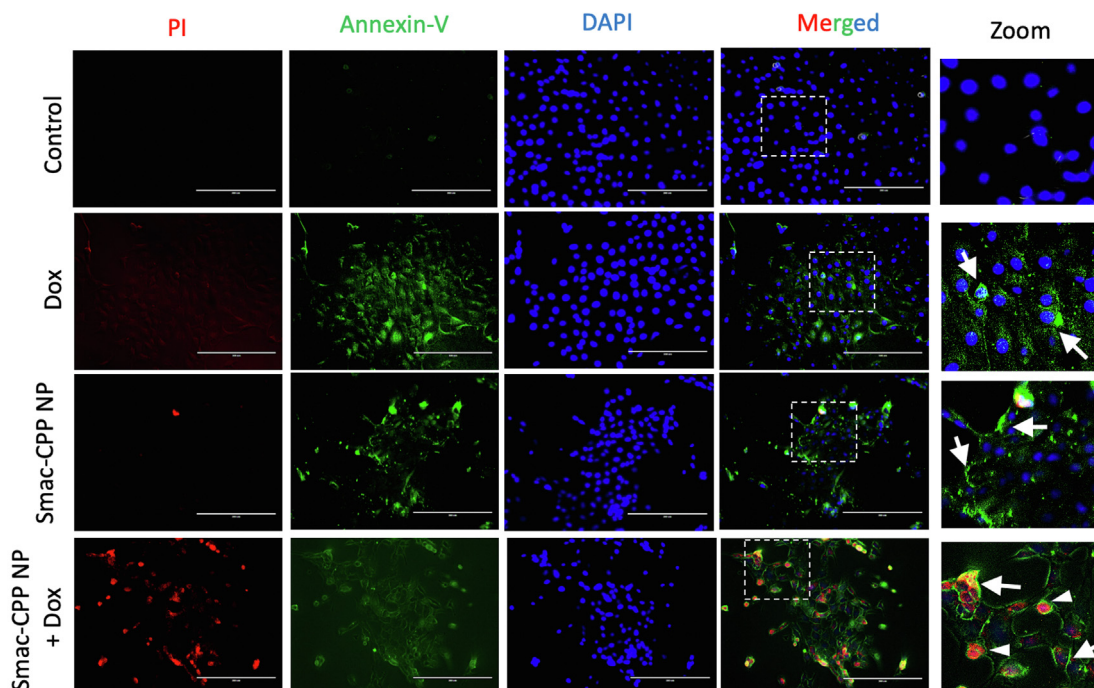


Fig. 5. Annexin-V staining to visualize early apoptosis of cells induced by Smac-CPP NPs. Representative fluorescence microscopic images showing Annexin V-FITC (green) and PI (red) staining after incubation of 4T1 cells with Dox (2 h), Smac-CPP NPs (16 h) or Dox (2 h) + Smac-CPP NPs (16 h). White arrows point towards annexin-V staining while arrowheads indicate to PI staining. $n = 3$. Scale bar: 50 μm .

doxorubicin induced both apoptosis (positive green stain) and cell death (red nuclei) (Fig. 5), indicating higher efficacy of the combination therapy. In the combined treatment images, the cells already shrunk and therefore the green color was only observed at the cell margin than large cytoplasm in only doxorubicin-treated cells. These data show that Smac-CPP NPs released the active peptide intracellularly which is in complete agreement with the data presented in Fig. 3C.

3.6. *In vivo* effects of Smac-CPP-loaded PLGA NPs in orthotopic 4T1 tumor model

The antitumor efficacy of Smac-CPP NPs *in vivo* in orthotopic 4T1 mouse breast tumor model was investigated. Treatments started about two weeks after inoculating tumor cells into the mammary glands of mice, when tumor reached a volume of around 100 mm^3 . In total 4 doses were administered intravenously via the tail vein at a dosing schedule of twice a week. Treatment with either Smac-CPP NPs or doxorubicin led to reduction of the tumor growth (Fig. 6A, B). Although the effect of the combination treatment of Smac-CPP NPs with doxorubicin tends to be higher than that of individual treatments, it did not reach statistical significant due to high inhibitory effect induced by free dox. No acute toxicity was seen with any of the treatments, as concluded from the body weight curves (Fig. 6C). Moreover, in literature it has been shown that the Smac peptide does not induce toxicity in healthy tissues (Fulda et al., 2002, Nat. Med. 8, 808–815), and therefore we expect no toxicity in liver and other organs.

Furthermore, the tumor tissues were examined for Ki-67 (a marker for cell proliferation, Urruticoechea et al., 2005) and cleaved caspase 3 (an apoptosis marker, Fernald and Kurokawa, 2013), respectively (Fig. 6D). Tumor samples of mice treated with Smac-CPP NPs or doxorubicin alone showed lower expression levels of Ki-67 but increased expression levels of cleaved caspase 3 compared to control mice. These data suggest that tumor cell proliferation was reduced and higher apoptosis was achieved with the combination treatment. As expected, the combination of Smac-CPP NPs and doxorubicin showed much less

Ki-67 positive cells and higher cleaved caspase positive cells, indicated by arrowheads (Fig. 6D). These results corresponds with the *in vitro* findings that combination of doxorubicin and Smac-CPP NPs led to both induced apoptosis and cell death (Figs. 4 and 5). Furthermore, we also do not rule out the uptake of NPs by other cells within the tumor microenvironment such as tumor-associated macrophages. The benefits of CPP binding to Smac peptide also showed in different studies. It was reported that 8-mer Smac peptide constructed with a CPP of antennapedia was successfully internalized into the cytoplasm of glioblastoma cell lines (Mizukawa et al., 2006). An arginine rich-CPP that bound to 7-mer-Smac peptide (Smac-N7) and combined with chemotherapeutic was also increased cellular uptake of the drug, thus enhanced its anti-tumor effect (Li et al., 2015). In addition, internalization of Tat-SmacN7 could promote RNA expression and caspase activation and sensitized the cancer cells to radiation to treat resistant human non-small cell lung cancer and esophageal cancer. (Chen et al., 2013).

4. Conclusions

The present study reports a novel strategy to deliver an apoptosis-inducing Smac-mimetic peptide by conjugating it with a CPP and then encapsulating the Smac-CPP peptide loaded PLGA nanoparticles. The results show that these passively delivered nanoparticles are able to induce apoptosis of tumor cells *in vitro* and inhibit tumor growth *in vivo*. Also, in *in vivo* study showed that co-delivering Smac-CPP peptide-loaded in PLGA NPs with an established chemotherapeutic agent (doxorubicin) resulted in a better therapeutic outcome.

Declaration of Competing Interest

The authors declare that they have no known competing financial interests or personal relationships that could have appeared to influence the work reported in this paper.

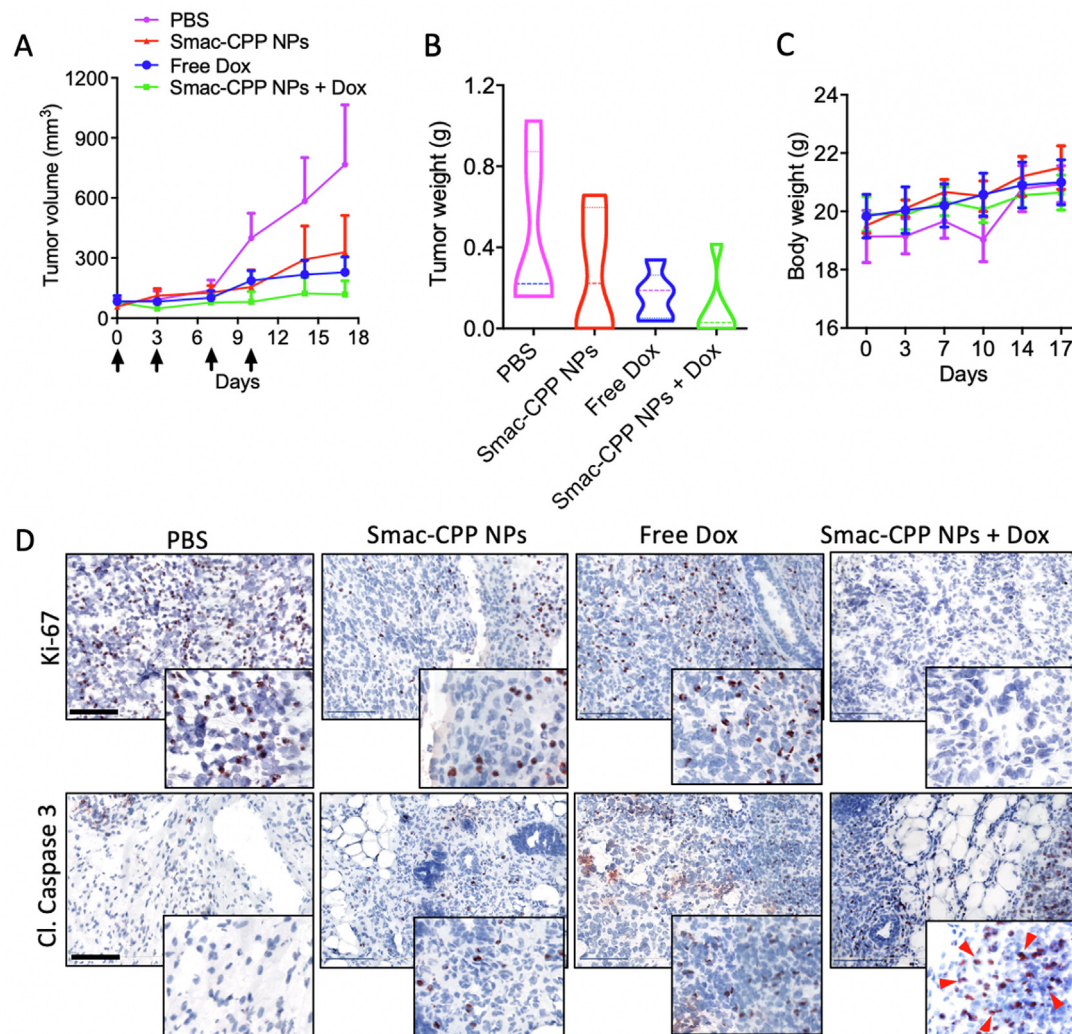


Fig. 6. Antitumor efficacy of Smac-CPP-loaded PLGA NPs in combination with doxorubicin in orthotopic 4T1 mouse breast tumor model. (A) Tumor growth curves showing the effect of different treatments including PBS, Smac-CPP NPs, free Dox, or Smac-CPP NPs + Dox. The dosing schedule is indicated by arrows. $N = 4$ to 6 mice per group, mean \pm SEM. (B) Tumor weight of the isolated tumors at the end of the experiment. (C) Body weight change during the treatments. (D) Immunohistochemical staining (red colored nuclei) of Ki-67 and cleaved caspase 3 on the tumor sections. Hematoxylin (violet color) was used as a counter staining. Red arrowheads indicate the positive nuclei for cleaved caspase 3. Scale bar: 100 µm.

Acknowledgements

Author thank Bettie Klomphaar for her technical support in performing animal experiments.

Funding statement

The project was funded by Directorate General of Higher Education (Direktorat Jenderal Pendidikan Tinggi, Kementerian Pendidikan dan Kebudayaan; DIKTI), Indonesia as Overseas Education Program to D.L.P.

Appendix A. Supplementary data

Supplementary data to this article can be found online at <https://doi.org/10.1016/j.ijpharm.2020.119535>.

References

Arnt, C.R., Chiorean, M.V., Heldebrant, M.P., Gores, G.J., Kaufmann, S.H., 2002. Synthetic Smac/DIABLO peptides enhance the effects of chemotherapeutic agents by

binding XIAP and cIAP1 *in situ*. J. Biol. Chem. 277, 44236–44243. <https://doi.org/10.1074/jbc.M207578200>.

Ausserlechner, M.J., Hagenbuchner, J., 2016. Mitochondrial survivin – an Achilles' heel in cancer chemoresistance. Mol. Cell Oncol. 3, e1076589-1-3. DOI:10.1080/23723556.2015. 1076589.

Balderstone, L.A., Dawson, J.C., Welman, A., Serrels, A., Wedge, S.R., Brunton, V.G., 2019. Development of a fluorescence-based cellular apoptosis reporter. Methods Appl. Fluores. 7, 1–13. <https://doi.org/10.1088/2050-6120/aac6f8>.

Barras, D., Widmann, C., 2011. Promises of apoptosis-inducing peptides in cancer therapeutics. Curr. Pharm. Biotechnol. 12, 1153–1165. <https://doi.org/10.2174/138920111796117337>.

Bruno, B.J., Miller, G.D., Lim, C.S., 2013. Basics and recent advances in peptide and protein drug delivery. Ther. Deliv. 4, 1443–1467. <https://doi.org/10.4155/tde.13.104>.

Chen, F.H., Xu, C., Du, L.Q., Wang, Y., Cao, J., Fu, Y., Guo, Y.T., Liu, Q., Fan, F.Y., 2013. Tat-SmacN7 induces radiosensitization in cancer cells through the activation of caspases and induction of apoptosis. Int. J. Oncol. 42, 985–992. <https://doi.org/10.3892/ijo.2013.1785>.

Cho, M., Sah, H., 2005. Formulation and process parameters affecting protein encapsulation into PLGA microspheres during ethyl acetate-based microencapsulation process. J. Microencapsul. 2, 1–12. <https://doi.org/10.1080/02652040400026269>.

Conner, S.D., Schmid, S.L., 2003. Regulated portals of entry into the cell. Nature 422, 37–44. <https://doi.org/10.1038/nature01451>.

Copolovici, D.M., Langel, K., Eriste, E., Langel, U., 2014. Cell-penetrating peptides: design, synthesis, and applications. ACS Nano 8, 1972–1994. <https://doi.org/10.1021/nm4057269>.

Danhier, F., Feron, O., Préat, V., 2010. To exploit the tumor microenvironment: passive

- and active tumor targeting of nanocarriers for anti-cancer drug delivery. *J. Control. Release* 148, 135–146. <https://doi.org/10.1016/j.jconrel.2010.08.027>.
- Danhier, F., Ansorena, E., Silva, J.M., Coco, R., Breton, A., Le, Pr  at V., 2012. PLGA-based nanoparticles: an overview of biomedical applications. *J. Control. Release* 161, 505–522. <https://doi.org/10.1016/j.jconrel.2012.01.043>.
- Du, A.W., Stenzel, M.H., 2014. Drug carriers for the delivery of therapeutic peptides. *Biomacromolecules* 15, 1097–1114. <https://doi.org/10.1021/bm500169p>.
- Du, L.Q., Wang, Y., Xu, C., Cao, J., Wang, Q., Zhao, H., Fan, F.Y., Wang, B., Katsube, T., Fan, S.J., Liu, Q., 2013. Radiation-sensitising effects of antennapedia proteins (ANTP) on tumour cells. *Int. J. Mol. Sci.* 14, 24087–24096. <https://doi.org/10.3390/ijms141224087>.
- El-Sayed, A., Futaki, S., Harashima, H., 2009. Delivery of macromolecules using arginine-rich cell-penetrating peptides: ways to overcome endosomal entrapment. *AAPS J.* 1, 13–22. <https://doi.org/10.1208/s12248-008-9071-2>.
- Faisant, N., Siepmann, J., Benoit, J.P., 2002. PLGA-based microparticles: elucidation of mechanisms and a new, simple mathematical model quantifying drug release. *Eur. J. Pharm. Sci.* 15, 355–366. [https://doi.org/10.1016/s0928-0987\(02\)00023-4](https://doi.org/10.1016/s0928-0987(02)00023-4).
- Fandy, T.E., Shankar, S., Srivastava, K.R., 2008. Smac/DIABLO enhances the therapeutic potential of chemotherapeutic drugs and irradiation, and sensitizes TRAIL-resistant breast cancer cells. *Mol. Cancer* 7, 60–70. <https://doi.org/10.1186/1476-4598-7-60>.
- Farkhani, S.M., Valizadeh, A., Karami, H., Mohammadi, S., Sohrabi, N., Badrzadeh, F., 2014. Cell penetrating peptides: efficient vectors for delivery of nanoparticles, nanocarriers, therapeutic and diagnostic molecules. *Peptides* 57, 78–94. <https://doi.org/10.1016/j.peptides.2014.04.015>.
- Fernald, K., Kurokawa, M., 2013. Evading apoptosis in anti-cancer. *Trends Cell Biol.* 23, 620–633. DOI:10.1016/j.tcb.2013.07.006.
- Fulda, S., 2010. Evasion of apoptosis as a cellular stress response in cancer. *Int. J. Biochem. Cell Biol.* 370835.
- Fulda, S., Wick, W., Weller, M., Debatin, K.M., 2002. Smac agonists sensitize for Apo2L/TRAIL- or anticancer drug-induced apoptosis and induce regression of malignant glioma *in vivo*. *Nat. Med.* 8, 808–815. <https://doi.org/10.1038/nm735>.
- Gao, Y., Li, M., Chen, B., Shen, Z., Guo, P., Wientjes, M.G., Au, J.L., 2013. Predictive models of diffusive nanoparticle transport in 3-dimensional tumor cell spheroids. *J. AAPS* 15, 816–831. <https://doi.org/10.1208/s12248-013-9478-2>.
- Gholizadeh, S., Kamps, J.A.A.M., Hennink, W.E., Kok, R.J., 2018. PLGA-PEG nanoparticles for targeted delivery of the mTOR/PI3kinase inhibitor dactolisib to inflamed endothelium. *Int. J. Pharm.* 548, 747–758. <https://doi.org/10.1016/j.jipharm.2017.10.032>.
- Giteau, A., Venier-Julienne, M.C., Aubert-Pou  ssel, A., Benoit, J.P., 2008. How to achieve sustained and complete protein release from PLGA-based microparticles? *Int. J. Pharm.* 350, 14–26. <https://doi.org/10.1016/j.jipharm.2007.11.012>.
- Gomes dos Rios, L., Lee, W., Svolos, M., Moir, L.M., Jaber, R., Windhab, N., Young, P.M., Traini, D., 2019. Nanotoxicologic effects of PLGA nanoparticles formulated with a cell-penetrating peptide: searching for a safe pDNA delivery system for the lungs. *Pharmaceutics* 11, 12. <https://doi.org/10.3390/pharmaceutics11010012>.
- Hirota, K., Dotya, A.C., Ackermann, R., Zhou, J., Olsen, K.F., Feng, M.R., Wang, Y., Choi, S., Qu, W., Schwendeman, A.S., Schwendeman, S.P., 2016. Characterizing release mechanisms of leuprolide acetate-loaded PLGA microspheres for IVIVC development I: *in vitro* evaluation. *J. Control. Release* 244, 302–313. <https://doi.org/10.1016/j.jconrel.2016.08.023>.
- Jain, A., Gulbake, A., Shilpi, S., Hurkat, P., Jain, S.K., 2013. Peptide and protein delivery using new drug delivery systems. *Crit Rev Ther Drug Carrier Syst.* 30, 293–329. <https://doi.org/10.1615/critrevtherdrugcarriersyst.2013006955>.
- Jain, R.K., Stylianopoulos, T., 2010. Delivering nanomedicine to solid tumors. *Nat. Rev. Clin. Oncol.* 7, 653–664. <https://doi.org/10.1038/nrclinonc.2010.139>.
- Jiao, C., Delaroche, D., Burlina, F., Alves, I.D., Chassaing, G., Sagan, S., 2009. Translocation and endocytosis for cell-penetrating peptide internalization. *J. Biol. Chem.* 284, 33957–33965. <https://doi.org/10.1074/jbc.m109.056309>.
- Joshi, V.B., Geary, S.M., Salem, A.K., 2013. Biodegradable particles as vaccine delivery systems: size matters. *AAPS J.* 15, 85–94. <https://doi.org/10.1208/s12248-012-9418-6>.
- Kocab, A.J., Duckett, C.S., 2016. Inhibitor of apoptosis proteins as intracellular signaling intermediates. *FEBS J.* 283, 221–231. <https://doi.org/10.1111/febs.13554>.
- Koppelhus, U., Awasthi, S.K., Zachar, V., Holst, H.U., Ebbesen, P., Nielsen, P.E., 2002. Cell-dependent differential cellular uptake of PNA, peptides, and PNA-peptide conjugates. *Antisense Nucl. acid Drug Dev.* 12, 51–63. <https://doi.org/10.1089/108729002760070795>.
- Li, M., Liu, P., Gao, G., Deng, J., Pan, Z., Wu, X., Xie, G., Yue, C., Cho, C.H., Ma, Y., Cai, L., 2015. Smac therapeutic peptide nanoparticles inducing apoptosis of cancer cells for combination chemotherapy with doxorubicin. *ACS Appl. Mater. Interfaces* 7, 8005–8012. <https://doi.org/10.1021/acsami.5b00329>.
- Li, Y., Peia, Y., Zhang, X., Gu, Z., Zhou, Z., Yuan, W., Zhou, J., Zhu, J., Gao, X., 2001. PEGylated PLGA nanoparticles as protein carriers: synthesis, preparation and bio-distribution in rats. *J. Control. Release* 71, 203–211. [https://doi.org/10.1016/s0168-3659\(01\)00218-8](https://doi.org/10.1016/s0168-3659(01)00218-8).
- Maeda, H., 2012. Macromolecular therapeutics in cancer treatment: The EPR effect and beyond. *J. Control. Release* 164, 138–144. <https://doi.org/10.1016/j.jconrel.2012.04.038>.
- Maeda, H., 2015. Toward a full understanding of the EPR effect in primary and metastatic tumors as well as issues related to its heterogeneity. *J. Control. Release* 91, 3–6. <https://doi.org/10.1016/j.addr.2015.01.002>.
- Mao, H.L., Pang, Y., Zhang, X., Yang, F., Zheng, J., Wang, Y., Liu, P., 2013. Smac peptide potentiates TRAIL- or paclitaxel-mediated ovarian cancer cell death *in vitro* and *in vivo*. *Oncol. Rep.* 29, 515–522. <https://doi.org/10.3892/or.2012.2132>.
- Margus, H., Padari, K., Pooga, M., 2012. Cell-penetrating peptides as versatile vehicles for oligonucleotide delivery. *Mol. Ther.* 20, 525–533. <https://doi.org/10.1038/mt.2011.284>.
- Mart  nez-Jothar, L., Doukouridou, S., Schifferers, R.M., Sastre Torano, J., Oliveira, S., van Nostrum, C.F., Hennink, W.E., 2018. Insights into maleimide-thiol conjugation chemistry: conditions for efficient surface functionalization of nanoparticles for receptor targeting. *J. Control Release* 282, 101–109. <https://doi.org/10.1016/j.jconrel.2018.03.002>.
- Mizukawa, K., Kawamura, A., Sasayama, T., Tanaka, K., Kamei, M., Sasaki, M., Kohmura, E., 2006. Synthetic Smac peptide enhances the effect of etoposide-induced apoptosis in human glioblastoma cell lines. *J. Neurooncol.* 77, 247–255. <https://doi.org/10.1007/s11060-005-9045-5>.
- Nakase, I., Tanaka

- [org/10.1002/bip.20989](https://doi.org/10.1002/bip.20989).
- Urruticoechea, A., Smith, I.E., Dowsett, M., 2005. Proliferation marker Ki-67 in early breast cancer. *J. Clin. Oncol.* 23, 7212–7220. <https://doi.org/10.1200/jco.2005.07.501>.
- van den Berg, A., Dowdy, S.F., Protein transduction domain delivery of therapeutic macromolecules. *Curr. Opin. Biotechnol.* 22, 888–893. DOI:10.1016/j.copbio.2011.03.008.
- Verderio, P., Bonetti, P., Colombo, M., Pandolfi, L., Prosperi, D., 2013. Intracellular drug release from curcumin-loaded PLGA nanoparticles induces G2/m block in breast cancer cells. *Biomacromolecules* 14, 672–682. <https://doi.org/10.1021/bm3017324>.
- Wilhelm, C., Billotey, C., Roger, J., Pons, J.N., Bacria, J.C., Gazeau, F., 2003. Intracellular uptake of anionic superparamagnetic nanoparticles as a function of their surface coating. *Biomaterials* 24, 1001–1011. [https://doi.org/10.1016/S0142-9612\(02\)00440-4](https://doi.org/10.1016/S0142-9612(02)00440-4).
- Xu, Q., Ensign, L.M., Boylan, N.J., Schön, A., Gong, X., Yang, J., Lamb, N.W., Cai, S., Yu, T., Freire, E., Hanes, 2015. Impact of surface polyethylene glycol (PEG) density on biodegradable nanoparticle transport in mucus *ex vivo* and distribution *in vivo*. *ACS Nano* 9, 9217–9227. <https://doi.org/10.1021/acs.nano.5b03876>.
- Yang, L., Mashima, T., Sato, S., Mochizuki, M., Sakamoto, H., Yamori, T., Oh-Hara, T., Tsuruo, T., 2003. Predominant suppression of apoptosome by inhibitor of apoptosis protein in non-small cell lung cancer H460 cells: therapeutic effect of a novel poly-arginine-conjugated Smac peptide. *Cancer Res.* 63, 831–837.